

FINITE ELEMENT ANALYSIS OF AN AXIAL FLUX HYBRID WIND GENERATOR

TIBERIU TUDORACHE¹, ION TRIFU¹

Key words: Permanent magnet hybrid wind generator, Finite element analysis, Electromagnetic field computation.

This paper deals with the 3D finite element analysis of an axial flux hybrid wind generator (HWG). The analyzed machine is designed to convert simultaneously the rotational mechanical energy into electrical energy and useful heat. The behavior and operation characteristics of the studied machine are estimated by a numerical analysis carried out using Flux ® software package.

1. INTRODUCTION

The efficient harnessing of renewable energies is a major preoccupation of scientists and engineers all around the globe. Among the renewable sources of energy, wind energy is one of the most relevant, with a high potential of conversion into other useful energies.

The wind turbines are usually used to produce electricity, this technology being a mature one. The key conversion element of a wind system is the wind generator which converts the rotational mechanical energy into electricity. The generators used for such purposes are typically of synchronous or asynchronous type [1–7].

This paper proposes an axial flux hybrid wind generator (HWG) able to convert the mechanical energy produced by a wind turbine simultaneously into electric energy and useful heat by cogeneration [8].

The configuration of the HWG is similar to a classical axial flux permanent magnet machine [9–11] but its stator magnetic core is made of a steel tube through which a thermal agent flows. The heat evacuated by the thermal agent can be used for domestic purpose. Due to the important heat quantity that can be evacuated by the thermal agent through forced convection the machine can be designed at higher current densities and saturation levels of the magnetic core. By its special construction the most part of the Joule and iron losses will be converted into useful heat by the thermal agent. Such a solution can lead to a very compact design and can operate at higher efficiency values by cogeneration than classical wind electric generators.

The advantages of the studied HWG are the following: compact design, high efficiency, ability to operate in important overload conditions by increasing the flow rate of the cooling fluid, small cost per unit of the output energy. The features and benefits of the machine recommend it for small power gearless wind turbines situated close to the end-user for small thermal losses (*e.g.* mounted on buildings roofs).

Due to its complexity the analysis of the device will be carried out using the Flux ® software package based on finite element (FE) method [12]. The purpose of the 3D numerical analysis presented in the paper is the proper design of the unconventional machine and the estimation with accuracy of the operation characteristics of the HWG in various conditions.

2. HWG DESCRIPTION

The studied HWG is a three-phase axial flux permanent magnet machine with two outer rotors and one inner toroidal slot-less stator, Fig. 1.

The proposed stator construction of the HWG leads to practical no cogging torque, allowing various “no. of poles - no. of coils” combinations.

The 30 stator coils (3 phases × 10 coils per phase) are made of insulated copper conductors and placed around the stator magnetic core made of toroidal steel-tube.

The permanent magnets (PMs) of NdFeB N30 type are placed on the two discoidal solid steel armatures and axially magnetized.

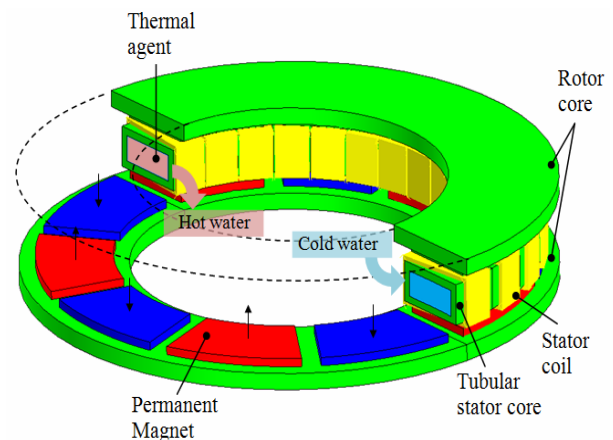


Fig. 1 – Main parts of the HWG.

The main electromagnetic and geometric data of the HWG are presented in Tables 1 and 2.

Table 1

Main electromagnetic data of HWG

Total rated power [kW]	2.2	No. of permanent magnets	20
Rated electric power [kW]	1.3	Magnetization direction	axial
Rated thermal power [kW]	0.9	Number of coils	10
Rated voltage [V]	120	Number of turns per coil	84
Rated current [A]	6.7	Resistance per phase [Ω]	≈ 5.5
Rated speed [rpm]	180	No of phases	3

Table 2

Main geometric data of HWG

Stator outer diameter [mm]	350
Stator inner diameter [mm]	230
Height of stator tube [mm]	40
Tube thickness [mm]	5
Magnets length [mm]	8
Inter-magnet distance [mm]	14.1

3. NUMERICAL MODEL OF HWG

The estimation of HWG operation characteristics will be carried out by 3D Finite Element (FE) numerical modeling of the machine. The numerical analysis supposes to solve transient electromagnetic field problems associated to different operation regimes of the studied HWG. The partial differential equations that should be solved are based on the electric vector potential T and total and reduced magnetic scalar potentials based on the general equation:

$$\mathbf{H} = -\text{grad } \Phi + \mathbf{T}, \tag{1}$$

where Φ is the magnetic scalar potential and \mathbf{H} is the magnetic field strength that is decomposed into two terms, the first one being irrotational $-\text{grad } \Phi$ [13].

By taking into account the 3D structure of the electromagnetic field of the machine the computation domain will be reduced 10 times and will include only 2 magnetic poles. The computation domain, the FE discretization and boundary conditions are shown in Fig. 2.

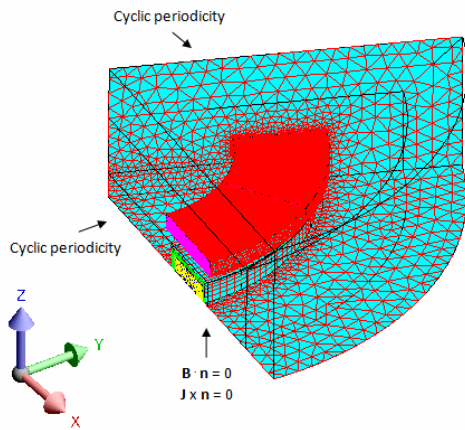


Fig. 2 – Computation domain, FE discretization and boundary conditions.

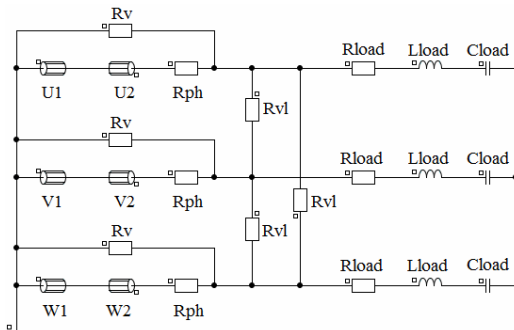


Fig. 3 – Circuit model associated to the electromagnetic field model of the HWG.

In order to analyze the operation of the HWG under electric load conditions the electromagnetic field model should be coupled with a circuit model of the device, Fig. 3. The proposed circuit include the coils per phase $U1, U2, \dots, W2$, the phase resistance R_{ph} , voltmeters R_v and R_{vl} and load components R_{load}, L_{load} and C_{load} .

4. FE ANALYSIS OF HWG UNDER NO-ELECTRIC LOAD CONDITION

The main purpose of the numerical analysis of the HWG is to size correctly the device so as to respect the main data and to estimate its operation characteristics.

The first study refers to the estimation of no-electric load operation of the machine. Based on the FE method a transient electromagnetic field problem associated to the HWG was solved, the obtained results being presented in Figs. 4–8.

In Fig. 4 is represented graphically the map of the magnetic flux density in the main physical regions of the computation domain in case of no-electric load. The numerical values are higher in the stator magnetic core region causing higher iron losses. However these losses are not dangerous in case of HWG since the most part of them will be converted into useful heat by means of the thermal agent flowing through the stator tube. The mean value of the magnetic flux density in the rotor core is within the recommended limits [14].

In Fig. 5 is presented the map of induced power density in the stator tube, one of the main thermal source of the device.

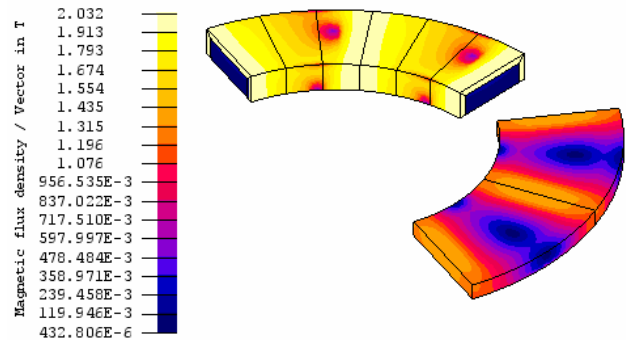


Fig. 4 – Map of magnetic flux density on the physical regions of the HWG.

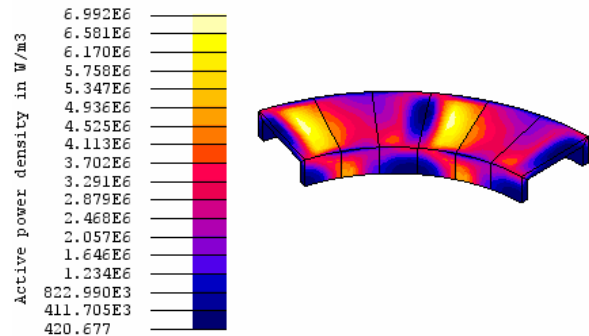


Fig. 5 – Map of induced power density in the stator tube of the HWG.

In Fig. 6 is presented the time variation of the line voltages across the stator terminals. We can notice that these waves are very close to perfect sine-waves.

The time variations of the power induced in the stator tube and the electromagnetic torque are shown in Figs. 7 and 8, respectively.

The ripples of the induced power are of about 0.82 % with respect to its mean value and the ripples of the electromagnetic torque are of 0.58 % with respect to the mean value. The amplitudes of these ripples are extremely small.

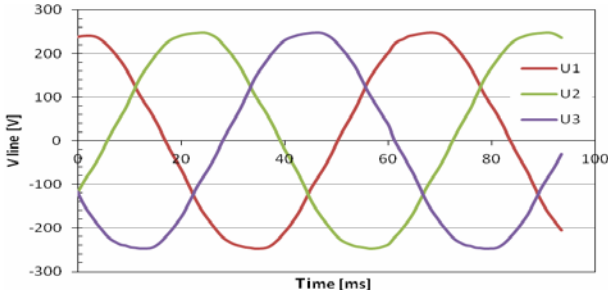


Fig. 6 – Time variation of line voltages of the HWG under no-electric load condition.

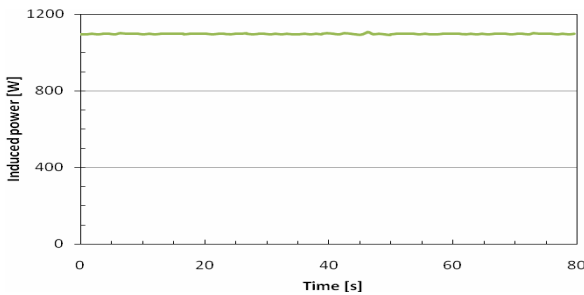


Fig. 7 – Time variation of the induced power of the HWG under no-electric load condition.

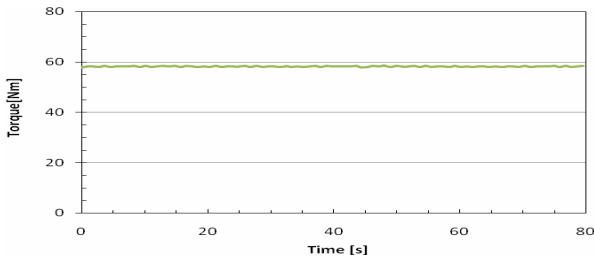


Fig. 8 – Time variation of electromagnetic torque of the HWG under no-electric load condition.

In Fig. 9 is shown the dependence between the mean electromagnetic torque and the rotational speed under no-electric load condition. This dependence is proved to be linear, the electromagnetic torque increasing from zero to about 59 Nm at rated speed (180 rpm).

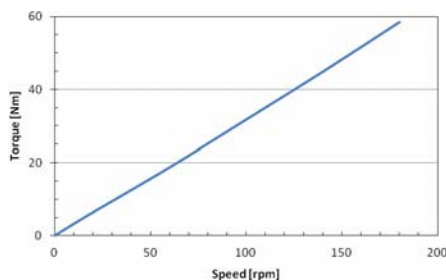


Fig. 9 – Electromagnetic torque versus generator speed under no-electric load condition.

5. OPERATION OF HWG UNDER ELECTRIC LOAD CONDITIONS

The estimation of the operation characteristics of the HWG under electric load was carried out by solving transient electromagnetic field problems associated to the machine operation in various load conditions. The numerical results obtained for the rated speed (180 rpm) of the HWG are presented in Figs. 10–13.

In Fig. 10 is presented the external characteristic of the HWG for purely resistive load. We can notice that from no-load to full electric load the output line voltage decreases from around 175 V to approximately 115 V (34.3 %).

Figure 11 presents the electric power $P_{electric}$, thermal power P_{th} and total power P_{total} versus electric current. The thermal power P_{th} is calculated as a sum between the induced power into the stator tube and the Joule losses developed into the windings. We can notice an approximately linear dependence of the total power on the line current.

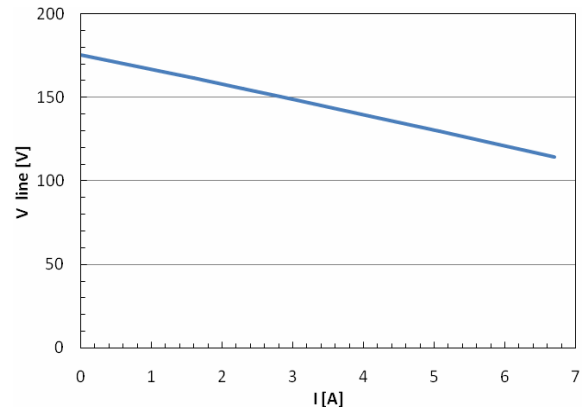


Fig. 10 – External characteristic of HWG for rated speed.

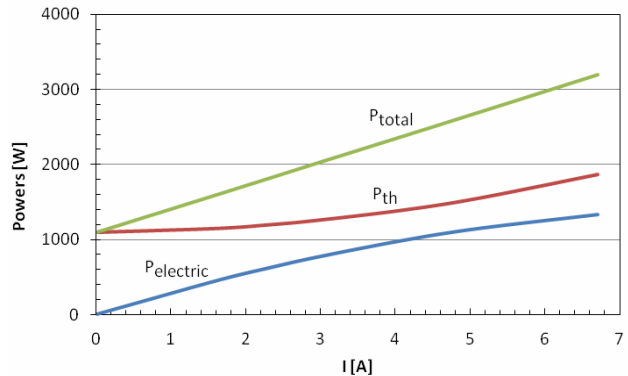


Fig. 11 – Electric, thermal and total power versus line current characteristic for rated speed.

The electromagnetic torque of the generator versus load current is shown in Fig. 12. We can notice that this dependence is practically linear increasing from about 59 Nm under no-electric load condition up to about 111 Nm in rated electric load condition.

The total power (electric and thermal) produced by the HWG versus load current for different rotational speed values is shown in Fig. 13. We can notice that the total power increases with the load current almost linearly and also with the rotational speed of the machine.

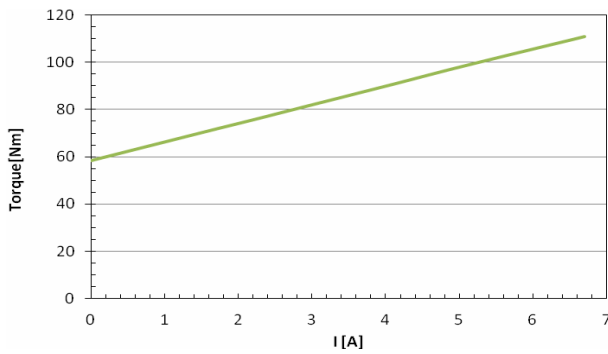


Fig. 12 – Electromagnetic torque versus line current characteristic for rated speed.

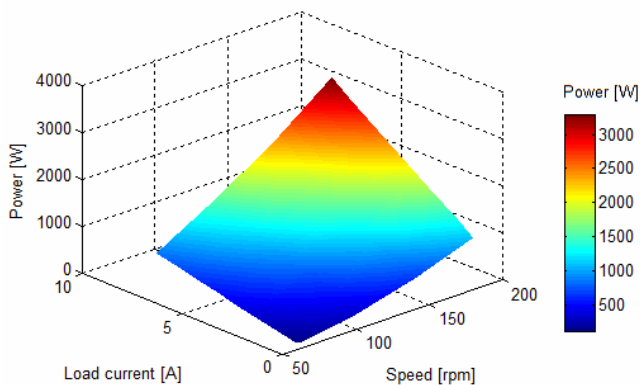


Fig. 13 – Total power versus line current characteristic for different rotational speed values.

6. CONCLUSIONS

This paper deals with the finite element analysis of a new concept of HWG able to convert rotational mechanical energy into electricity and thermal power, the first destination of the device being the roof mounted wind turbines.

The numerical analysis allowed us to design properly the unconventional machine and to estimate its main operation characteristics under no-electric load conditions as well as under various electric load conditions.

The estimated characteristics of the HWG are useful to match the generator to the primary mover (wind turbine).

The 3D numerical simulations proved also that the ratio between the electric and thermal power produced by the machine is an important design parameter that has a significant influence on the HWG overall size.

ACKNOWLEDGEMENTS

This paper was elaborated in the framework of the Bridge Grant Programme – PNCDI III, financed by MEN – UEFISCDI, project no. 68BG/2016.

Received on April 29, 2017

REFERENCES

1. L. Barote, C. Marinescu, *Modeling and Operational Testing of an Isolated Variable Speed PMSG Wind Turbine with Battery Energy Storage*, Advances in Electrical and Computer Engineering Journal, **12**, 2, pp. 81–88, 2012.
2. S. Tamalouzt, K. Idjdarene, T. Rekioua, R. Abdessemed, *Direct Torque Control of Wind Turbine Driven Doubly Fed Induction Generator*, Rev. Roum. Sci. Techn. – Électrotechn. et Énerg., **61**, 3, pp. 244–249, 2016.
3. A. Maafa, D. Aouzellag, K. Ghedamsi, R. Abdessemed, *Cascaded Doubly Fed Induction Generator with Variable Pitch Control System*, Rev. Roum. Sci. Techn. – Électrotechn. et Énerg., **61**, 4, pp. 361–366, 2016.
4. Y. Duan, R.G. Harley, *Present and future trends in wind turbine generator designs*, Proc. of Power Electronics and Machines in Wind Applications (PEMWA 2009), Lincoln, 2009.
5. V.V. Mehtre, S.G. Desai, D.S. Bankar, *Analysis of a Doubly Fed induction generator based wind farm*, Proc. of IEEE Technological Innovations in ICT for Agriculture and Rural Development (TIAR 2016), Chennai, 2016.
6. N. Karakasis, N. Jabbour, E. Tsioumas, C. Mademlis, *Efficiency increase in a wind system with Doubly Fed Induction Generator*, Proc. of 42nd IEEE Annual Conference of the Industrial Electronics Society, (IECON 2016), Florence, 2016.
7. T. Tudorache, L. Melcescu, S.V. Paturca, *Finite Element Analysis of Self-Excited Induction Generator for Isolated Small Power Wind Turbines*, Proc. of the International Conference on Clean Electrical Power (ICCEP 2007), Capri, 2007, pp. 656–661.
8. Patent demand No. 00006/2017, *Hybrid Axial Flux Wind Generator*, OSIM, January 2017.
9. F. Marignetti, R. Di Stefano, Y. Coia, *Analysis of Axial Flux PM Machines Including Stator and Rotor Core Losses*, Proc. of the 34th IEEE Annual Conference of Industrial Electronics (IECON 2008), Orlando, 2008, pp. 2035–2040.
10. R. Di Stefano, F. Marignetti, *A Comparison BETWEEN Soft Magnetic Cores for Axial Flux PM Synchronous Machines*, Proc. of XXth International Conference on Electrical Machines (ICEM), Marseille, 2012, pp. 1922–1927.
11. A. Mahmoudi, H.W. Ping, N.A. Rahim, *A comparison between the TORUS and AFIR axial-flux permanent-magnet machine using finite element analysis*, Proc. of the IEEE International Electric Machines & Drives Conference (IEMDC), Niagara Falls, 2011, pp. 242–247.
12. CEDRAT, *User guide Flux® 12*, Volume 3, 2015.
13. L. Melcescu, T. Tudorache, M. Popescu, *Numerical Analysis of a Yokeless Axial Flux Permanent Magnet Machine* (in Romanian), Proc. of Current Topics and Perspectives in Electrical Machines Symposium (SME 2016), Bucharest, 2016.
14. I. Cioc, C. Nica, *Design of Electrical Machines* (in Romanian), Edit. Didactică și Pedagogică, Bucharest, 1994.